

Soliton lattice structure and midgap band in nearly commensurate charge-density-wave states

Masahiro Nakano and Kazushige Machida

Department of Physics, Kyoto University, Kyoto 606, Japan

(Received 17 July 1985; revised manuscript received 18 November 1985)

The incommensurate charge-density-wave (CDW) states for systems with a nearly-half-filled, a nearly-third-filled and a nearly-quarter-filled band are investigated theoretically by solving the Fröhlich model in one dimension within a mean-field approximation. The Hamiltonian matrices with sizes as large as 100×100 are numerically diagonalized in momentum space in a self-consistent manner, taking into account all higher harmonics. The stable CDW states are thus determined, yielding the energy-gap structure, the electron-density modulation, the order parameters with various higher harmonic components, and the degree of localization of the eigenfunctions. It is shown that the midgap band inside the main Peierls gap always appears in nearly commensurate CDW states. This is attributed to the soliton (or kink) lattice structure of the electron-density modulation. A universal form of the electron-density modulation is deduced in the commensurate limit. Peculiar peaks found in the recent absorption experiment on orthorhombic TaS_3 are interpreted in terms of the midgap band. Possible experiments on other quasi-one-dimensional CDW materials such as $\text{K}_{0.3}\text{MoO}_3$ are proposed.

I. INTRODUCTION

Much attention has been recently focused on incommensurate states in various materials from dielectrics to metals.¹ In particular, the charge-density-wave (CDW) states in quasi-one-dimensional materials such as TaS_3 , NbSe_3 , $(\text{TaSe}_4)_2\text{I}$, and $\text{K}_{0.3}\text{MoO}_3$ have attracted much interest in connection with their non-Ohmic conduction mechanism.² In spite of intensive theoretical and experimental efforts, a most fundamental property of the ordered state, namely the energy-gap structure of the incommensurate CDW (ICDW), has not yet been fully elucidated, partly because of the difficulty in making a good sample.

Recently, a remarkable experiment on orthorhombic TaS_3 has been reported.³ This experiment strongly indicates that the nearly-quarter-filled commensurate CDW state^{4,5} possesses a midgap band inside the main Peierls gap.

There has been much theoretical work⁶⁻²⁴ on an ICDW system with a nearly-half-filled band (commensurability index $n=2$),⁶⁻¹¹ a nearly-third-filled band ($n=3$),¹²⁻²⁰ and a nearly-quarter-filled band ($n=4$).^{21,22} The nearly-half-filled case has been most extensively studied. An exact solution within the mean-field theory of the Fröhlich model is known.⁶⁻⁹ For the other electron-filling fractions,²³ however, the detailed properties of the ICDW have not yet been investigated. In particular, the energy-gap structure near the Fermi level in such a nearly commensurate CDW state has not been studied thoroughly.

Here we study the ICDW state in systems with a nearly-half-filled, a nearly-third-filled, and a nearly-quarter-filled band, aiming at finding general properties of the nearly commensurate CDW state. Starting with the standard model for the Peierls transition in one dimension, we apply a mean-field approximation to it. We

properly take into account all higher harmonics and diagonalize the mean-field Hamiltonian in a self-consistent manner. The momentum- (or wave-number-) space representation of the Hamiltonian is employed to perform numerical diagonalization. It is quite easy to draw information of the global features of a system such as the band structure, or the soliton lattice structure of the electron-density modulation, in this representation, while the real-space representation used by Su and Schrieffer¹² and Ono *et al.*²⁰ is advantageous in obtaining local properties of the CDW state, such as the one-soliton profile as a localized object in the Su-Schrieffer-Heeger (SSH) model.²⁵ Thus, these two approaches are complementary. We emphasize, however, that the advantage of our momentum-space approach lies in the facts that (1) we can effectively treat an infinite system with various unit-cell sizes and, thus, (2) we can obtain the most stable state of the CDW with the periodically modulated structure, or the soliton lattice structure and associated bands. It is interesting to compare our work with that of Le Daëron and Aubry,²⁶ who have done a similar self-consistent calculation in real space and discussed the band structure from a different point of view in connection with the electron-localization problem.²⁷

The present work²⁸ is a natural extension of the work by Kotani¹⁰ and Kotani and Harada²³ to higher commensurate cases, enabling us to yield information on the "nearly commensurate" CDW state. We only treat higher commensurate states and approach a true incommensurate state by increasing the commensurability index and examining systematic changes of the higher commensurate states. This approach might be justified when we consider a real system because, in the existing experiments, it is practically impossible to see the difference between a true incommensurate state and a higher commensurate state.

In the next section, we give a formulation of the prob-

lem based on the mean-field Fröhlich model in one dimension. The results of the self-consistent calculations are shown in Sec. III, mainly for the third-filled-band and quarter-filled-band cases, because the half-filled-band case has been extensively studied numerically and analytically. We devote Sec. IV to discussion of the experimental relevance and the validity of our theory. Summary and conclusion are given in the last section. Throughout this paper, we confine our arguments to the ground state ($T=0$).

II. FORMULATION

We start with the Fröhlich Hamiltonian in one dimension and treat it in momentum space:

$$H = \sum_k \epsilon_k c_k^\dagger c_k + \sum_k \omega_k b_k^\dagger b_k + \frac{1}{\sqrt{N}} \sum_{k,q} g_q (b_q + b_{-q}^\dagger) c_k^\dagger c_{k-q}, \quad (2.1)$$

where c_k^\dagger (b_k^\dagger) is the creation operator of an electron (phonon) with wave number k . The energy spectrum of the electron (phonon) system is ϵ_k (ω_k). The electron-phonon interaction in the third term comes from the coupling between the electron charge density $\rho_q = \sum_k c_k^\dagger c_{k+q}$ with wave number q and the ionic displacement. Its coupling constant is denoted by g_q . N is the total number of ion sites. We have neglected the electron spin. The electron density ρ_n at the n th site is given by

$$\rho_n = \frac{1}{N} \sum_k \rho_q e^{iqn}. \quad (2.2)$$

The ionic displacement u_n at the n th site is expressed in terms of the phonon operators by

$$u_n = \frac{1}{\sqrt{N}} \sum_q \frac{1}{(2M\omega_q)^{1/2}} (b_q + b_{-q}^\dagger) e^{iqn}, \quad (2.3)$$

where M is an ion mass.

Applying the mean-field approximation to Eq. (2.1), we obtain

$$H = H_{\text{el}} + H_{\text{ph}} - \sum_k \Delta_k \langle \rho_k \rangle, \quad (2.4)$$

$$H_{\text{el}} = \sum_k \epsilon_k c_k^\dagger c_k + \sum_k \Delta_k \rho_{-k}, \quad (2.5)$$

$$H_{\text{ph}} = \sum_k \omega_k b_k^\dagger b_k + \frac{1}{\sqrt{N}} \sum_q g_q \langle \rho_{-k} \rangle (b_q + b_{-q}^\dagger), \quad (2.6)$$

with the order parameter, which is assumed to be real,

$$\Delta_k = \frac{1}{\sqrt{N}} g_k (\langle b_k \rangle + \langle b_{-k}^\dagger \rangle), \quad (2.7)$$

where $\langle \dots \rangle$ is the expectation value. The mean-field Hamiltonian H_{el} (H_{ph}) describes the electron (phonon) motion under a given lattice distortion (an electron-density modulation). The diagonalization of the phonon Hamiltonian H_{ph} in Eq. (2.6) readily yields a self-consistent equation for the order parameter:

$$\Delta_k = - \frac{2 |g_k|^2}{N \omega_k} \langle \rho_k \rangle. \quad (2.8)$$

The mean-field approximation for phonon variables is equivalent to the adiabatic approximation.

Let us consider the system with electron number ν per site ($0 < \nu < 1$). The lattice distortion, due to the Peierls instability, described by the fundamental wave number $Q = 2k_F$ (the Fermi wave number is $k_F = \pi\nu/a$ and a is the lattice constant), which is a most effective nesting wave number, spontaneously occurs in the ground state. This lattice distortion, or the primary order parameter Δ_Q , necessarily induces the distortion with higher harmonics (Δ_{2Q} , Δ_{3Q} , etc.) generated through the self-consistent condition (2.7). Thus the effective mean-field electron Hamiltonian, in which all higher harmonics of the order parameter are taken into account, is written as

$$H_{\text{el}} = \sum_k \epsilon_k c_k^\dagger c_k + \sum_{l=1,2,\dots}^{\infty} \Delta_{lQ} \rho_{-lQ}. \quad (2.9)$$

The self-consistent condition is now given by

$$\Delta_{lQ} = - \frac{2 |g_{lQ}|^2}{N \omega_{lQ}} \langle \rho_{lQ} \rangle \quad (2.10)$$

with $l = 1, 2, 3, \dots, \infty$.

When ν is rational, i.e. $\nu = m/n$, where n and m are prime to each other, the problem is reduced to diagonalizing an $n \times n$ Hamiltonian matrix which is constructed from Eq. (2.9). We call n the commensurability index. The incommensurate state is characterized by an irrational ν . We approximate it by the commensurate state with a high commensurability index n as mentioned in Sec. I.

Our numerical calculations are performed by a simple iteration method which diagonalizes Eq. (2.9) under the self-consistent condition Eq. (2.10): We first assume a set of initial values Δ_{lQ} ($l = 1, 2, \dots, n$). Then diagonalizing the $n \times n$ Hamiltonian matrix to obtain the eigenvalues and eigenfunctions for certain points (about 1000 points) in the first Brillouin zone of the undistorted system, we obtain a new set of Δ_{lQ} and substitute these values into Eq. (2.9) to check the self-consistency. This step is repeated until self-consistency is attained. The resulting self-consistent solution, which consists of the values of Δ_{lQ} , the eigenvalues, and the corresponding wave functions, provides information concerning the ground state of our system, such as the spatial variation of the electron density, the band structure, etc.

We have assumed in the following that the energy band ϵ_k is given by

$$\epsilon_k = - \cos k, \quad (2.11)$$

where the energy unit is scaled by twice the transfer integral $2t$ in the tight-binding model; thus the unperturbed band is spread over $-1 \leq E \leq 1$. The length scale is measured by the lattice constant a . The dimensionless electron-phonon coupling constant is assumed to be independent of the wave number for the convenience of computation, that is,

$$\alpha^2 = \frac{2 |g_{lQ}|^2}{\omega_{lQ}}, \quad (2.12)$$

although it is not difficult to extend it to k -dependent cases in our formulation (see Sec. IV for detail). The

Hamiltonian to be diagonalized is now

$$H_{el} = - \sum_k c_k^\dagger c_k \cos k + \sum_{l=1}^n \Delta_{lQ} \rho_{-lQ} \quad (2.13)$$

with

$$\Delta_{lQ} = - \frac{\alpha^2}{N} \langle \rho_{lQ} \rangle. \quad (2.14)$$

We consider the systems with a nearly-half-filled ($n=2$), nearly-third-filled ($n=3$), and nearly-quarter-filled ($n=4$) band, where n is defined by $\nu=(1/n)(1+\delta)$, that is, we focus on nearly commensurate states. The deviation from the lower commensurate state is characterized by δ . To approach a nearly commensurate situation, δ has to be small enough. The maximum size of the matrix we have treated is about 100; therefore the smallest value of δ is the order of 0.01. In this case, our calculation is effectively of an infinite system with an effective unit cell of size about 100 sites. We have employed the periodic boundary condition.

III. SELF-CONSISTENT CALCULATION

According to the formulation mentioned above, we have performed numerical diagonalization of the Hamiltonian matrix Eq. (2.13) for various values of the coupling constant α and the derivation δ from a nearby commensurate state. The results of the self-consistent calculation are presented mainly for the third- and quarter-filled cases, including the overall band structure, the CDW energy-gap structure, electron-density modulation, and eigenfunctions.

A. Overall band structure

When an electron band is just a third- (quarter-) filled, the trimerized (quadrimerized) lattice distortion occurs in the ground state because of the Peierls instability. The fundamental wave number $Q=2\pi/3$ ($Q=2\pi/4$) corresponding to $2k_F$ characterizes the periodicity of the distortion and the concomitant electron-density modulation. We show schematically the relevant wave numbers for the Peierls distortion in Fig. 1 for both third- and quarter-filled cases, where $2Q$ ($3Q$) is equivalent to Q in the former (latter) case. The overall band in the perfect trimerized (quadrimerized) state is split into three (four) bands by opening up two (three) Peierls gaps, as displayed in Fig. 2. The lowest-energy band is occupied and the others are empty in one third- (quarter-) filled case.

The band structure in the nearly-third-filled case is shown in Fig. 3. The band is split into three main bands as in the perfect trimerized case in Fig. 2. However, inside each gap the midgap states appear, as is clearly seen in Fig. 4 where the enlarged figures near the Fermi level are shown. It is observed from Fig. 3 that as the coupling constant α increases, the Peierls gaps become wider and the relative position of the midgap band approaches the nearby band (conduction or valence band). The corresponding figures in the nearly-quarter-filled case are shown in Figs. 5 and 6. We can observe a similar energy-gap structure; the midgap band split off from the valence

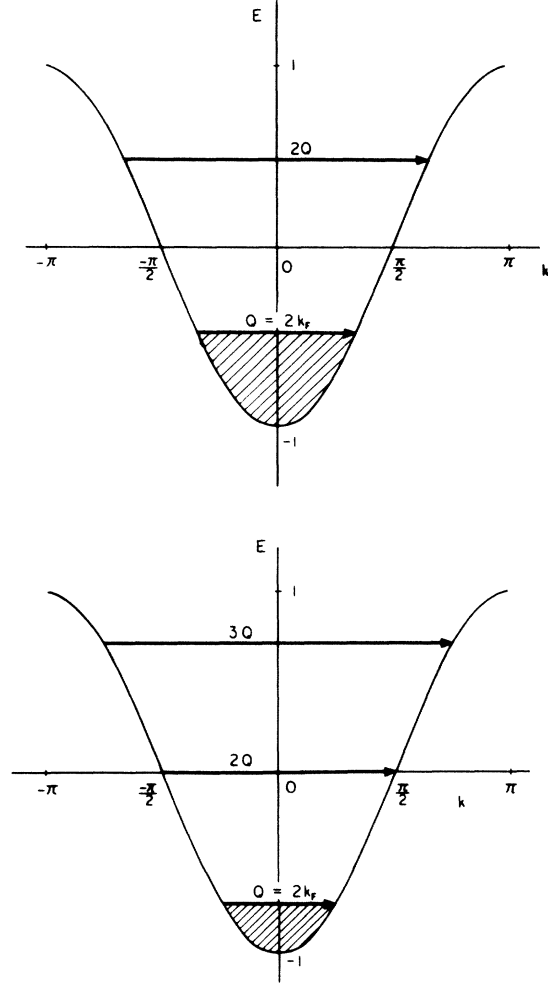


FIG. 1. Relevant wave numbers Q , $2Q$, and $3Q$ in (a) the one-third-filled case and (b) one-quarter-filled case. These wave numbers induce the Peierls gaps in the cosine band. The hatched region is occupied. Note that $2Q$ ($3Q$) is equivalent to Q in the perfect third- (quarter-) filled case.

(or conduction) band appears inside every main Peierls gap.

B. Midgap band

The traces of the top of the valence band, the bottom of the conduction band, and the edges of the midgap band are depicted in Fig. 7 as a function of the deviation δ from the nearby commensurate states. As $|\delta|$ becomes small or the system approaches the commensurate state, the width of the midgap band becomes narrower, tending to the midgap level. The limit corresponds to the so-called soliton level. The position of the midgap band relative to the main gap near the Fermi level is not symmetric about $\delta=0$, but inversion symmetric about the center of the main gap in the third- and quarter-filled cases. The limits of the position of the midgap band in the third-filled case are approximately $0.1 \times$ the main Peierls gap from the valence (conduction) band when $\delta < 0$ ($\delta > 0$),

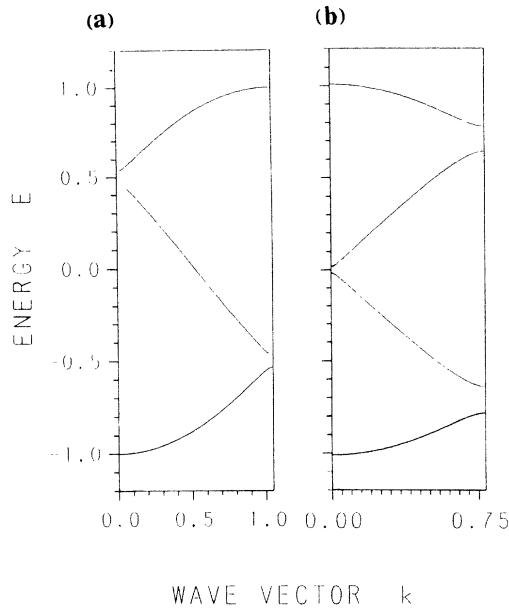


FIG. 2. Band structures in the perfect (a) third-filled and (b) quarter-filled cases drawn in the reduced-zone schema. The band is split into three (four) bands and the two (three) Peierls gaps appear in the third- (quarter-) filled case ($\alpha=1.08$).

which roughly coincides with the energy level of the one-soliton state ($\pm \frac{2}{3}$ soliton) evaluated by Ono *et al.*²⁰ As the commensurability index increases, the position of the midgap band is pushed toward the nearest main band.

C. Order parameters

Figure 8 shows the primary order parameter Δ_Q as a function of the electron filling for a fixed value of α ($=1.0$). The breaks of the smooth curve occur at electron filling fractions of $\frac{1}{2}$, $\frac{1}{3}$, and $\frac{1}{4}$. The detailed figure near the third-filled case reveals $\lim_{Q \rightarrow 2\pi/3} \Delta_Q \cong 0.83\Delta_C$, or $\Delta_Q \rightarrow 0.83\Delta_C$ as $Q \rightarrow 2\pi/3$ as is seen from Fig. 9. The corresponding ratios of the limiting values to the commensurate ones are ~ 0.9 and ~ 0.64 for the quarter- and half-filled cases, respectively. These limiting values are found to be independent of the coupling constant α . This is consistent with the analytical calculations as is shown later.

The relative amplitudes of various harmonics are exhibited in Fig. 10 near the commensurate states. The magnitudes of $\tilde{\Delta}_{5Q}$ and $\tilde{\Delta}_{3Q}$ ($\tilde{\Delta}_{5Q}$ and $\tilde{\Delta}_{4Q}$) are reversed at $|\delta_{cr}| \sim 0.02$ ($|\delta_{cr}| \sim 0.01$) for the third- (quarter-) filled cases, signaling that inside this region the nearly commensurate state is realized where the higher harmonics are essential in forming the CDW. The crossover region of δ for the quarter-filled cases is apparently narrower than those for the half- and third-filled cases, as is seen from Figs. 10(a)–10(c).

As the system approaches the commensurate state ($\delta \rightarrow 0$) in the third-filled case the $(3l \pm 1)$ th harmonics grow while the $3l$ th harmonics decrease, because the wave number $(3l \pm 1)Q$ ($l=1,2,3,\dots$) becomes relevant in forming the energy gap near the Fermi level and thus the corresponding order parameters should grow (see Fig. 1).

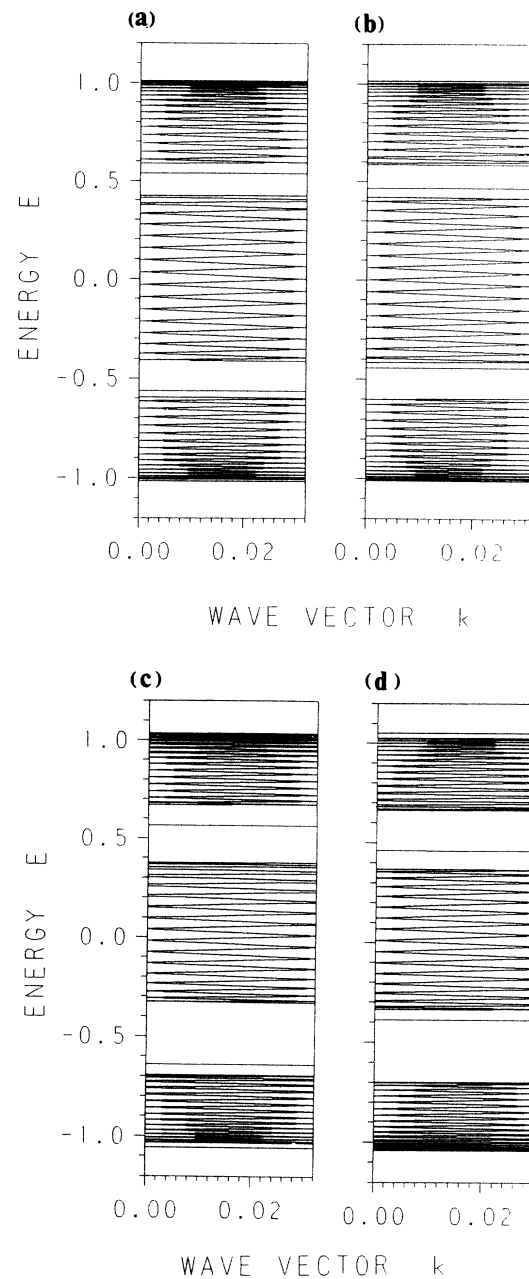


FIG. 3. Overall band structure in the nearly-third-filled case. (a) $\alpha=1.08$, $\delta=\frac{1}{98}$; (b) $\alpha=1.08$, $\delta=-\frac{1}{100}$; (c) $\alpha=1.15$, $\delta=\frac{1}{98}$; (d) $\alpha=1.15$, $\delta=-\frac{1}{100}$. The band is mainly split into three parts. Note, however, that inside each main gap a sharp energy band can be seen. The states below $E=-0.5$ are occupied. As α decreases, the position of the midgap band shifts toward the center of the main gap.

Similarly, in the quarter-filled case, the $(4l \pm 1)$ th harmonics grow while the $4l$ th harmonics decrease and become irrelevant and the $(4l \pm 2)$ th harmonics stay constant.

As is estimated from Fig. 10, all the limiting values of the relevant harmonics toward the commensurate states are approximately given by

$$\lim |\Delta_{nQ}| = \Delta_C / n. \quad (3.1)$$

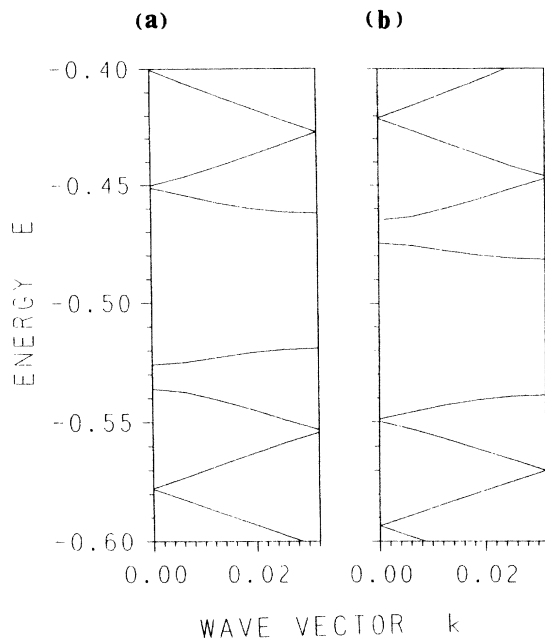


FIG. 4. Band structure near the Fermi level. It is clearly seen that inside the main gap a sharp band appears. It is isolated from the conduction band above $E > -0.47$ and the valence band below $E < -0.53$. (a) $\alpha=1.0$, $\delta=\frac{1}{98}$; (b) $\alpha=1.0$, $\delta=-\frac{1}{100}$.

This formula is valid for the third-, quarter-, and half-filled cases and holds for $\alpha=1.08$ and 1.15 within a certain numerical uncertainty. From these limiting behaviors, we can deduce a plausible form of the order pa-

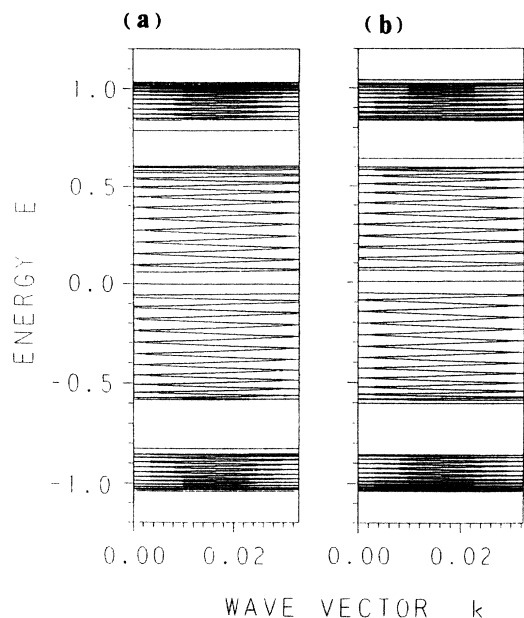


FIG. 5. Band structure in the nearly-quarter-filled case. (a) $\alpha=1.15$, $\delta=\frac{1}{95}$; (b) $\alpha=1.15$, $\delta=-\frac{1}{97}$. The band is mainly split into four bands. Note that inside each main gap a sharp energy band can be seen. The states below $E = -0.7$ are occupied.

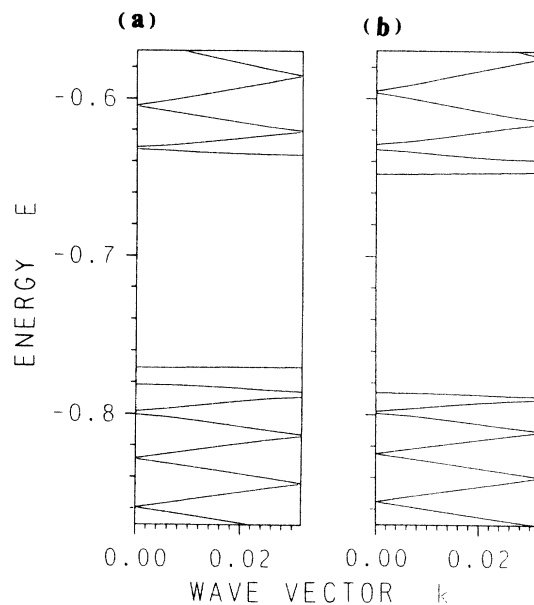


FIG. 6. Band structure near the Fermi level. It is seen that inside the main gap a sharp band appears which is isolated from the conduction band above $E > -0.64$ and the valence band below $E < -0.78$. (a) $\alpha=1.08$, $\delta=\frac{1}{95}$; (b) $\alpha=1.08$, $\delta=-\frac{1}{97}$.

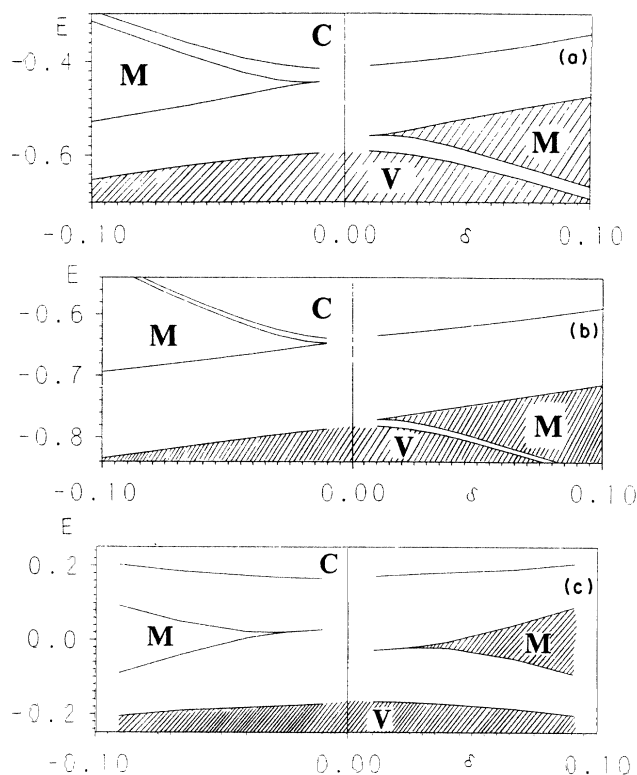


FIG. 7. Traces of the energy-band edges near the Fermi level as a function of the deviation δ from the commensurate state. The hatched regions are occupied. *V*, *M*, and *C* stand for the valence, midgap, and conduction bands, respectively. (a) The third-filled case ($\alpha=1.08$), (b) the quarter-filled case ($\alpha=1.08$), and (c) the half-filled case ($\alpha=1.0$). The tending limits of the midgap band from $\delta > 0$ and $\delta < 0$ toward $\delta \rightarrow 0$ are different in (a) and (b) and nearly the same in (c). Note that as the commensurability index increases, the midgap band becomes closer to the main band.

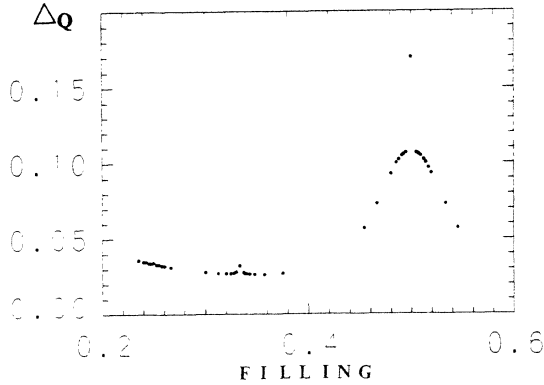


FIG. 8. Variation of the fundamental order parameter Δ_Q as a function of the electron filling ($\alpha=1.0$).

parameter in nearly commensurate CDW states: A combination of the step functions shown in Fig. 11 turns²⁹ out to give exactly the same Fourier coefficients as in Eq. (3.1). These analytical limiting forms, in turn, give the tending limits of the primary order parameters: $\Delta_Q/\Delta_C=2/\pi$ ($\frac{1}{2}$ -filled case), $3\sqrt{3}/2\pi$ ($\frac{1}{3}$ -filled case), and $2\sqrt{2}/\pi$ ($\frac{1}{4}$ -filled case). Our extrapolated values mentioned above agree with these values. A correct analytical solution which remains unknown at present for the $\frac{1}{3}$ - and $\frac{1}{4}$ -filled cases must recover these limiting forms.

D. Electron-density modulation

We show the electron density as a function of the lattice site in Fig. 12 for the $\frac{1}{3}$ -filled case and in Fig. 13 for the $\frac{1}{4}$ -filled case. In the $\frac{1}{3}$ -filled case ($\frac{1}{4}$ -filled case), the kink which connects the threefold (fourfold) degenerate ground states becomes evident as α increases. Between kinks, which are regularly placed to form a kink (or soliton) lattice, an almost perfect trimerized (quadrimerized) electron-density modulation is realized. For the $\frac{1}{3}$ -filled case the density-modulation pattern $+--$ changes into a $--+$ pattern after passing a kink for $\delta>0$. For $\delta<0$,

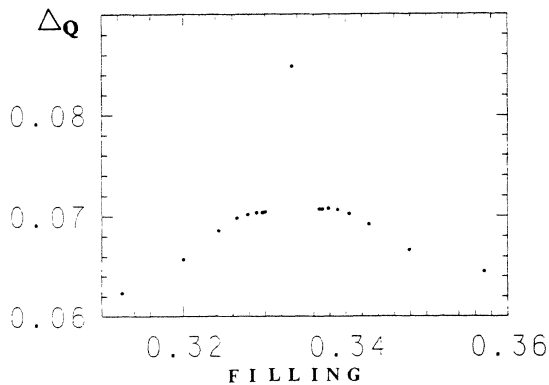


FIG. 9. Detailed figure of the variation of the fundamental order parameter Δ_Q as a function of the electron filling near the third-filled case. The isolated point corresponds to the perfect third-filled case ($\alpha=1.08$).

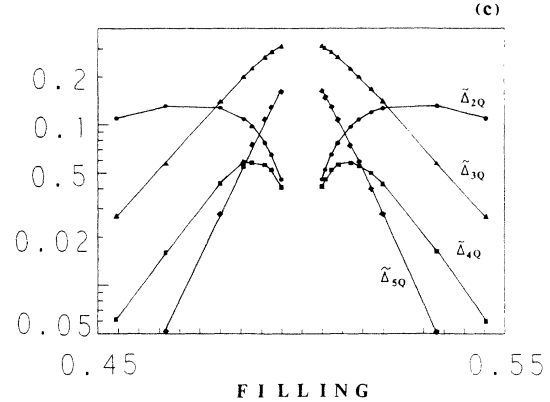
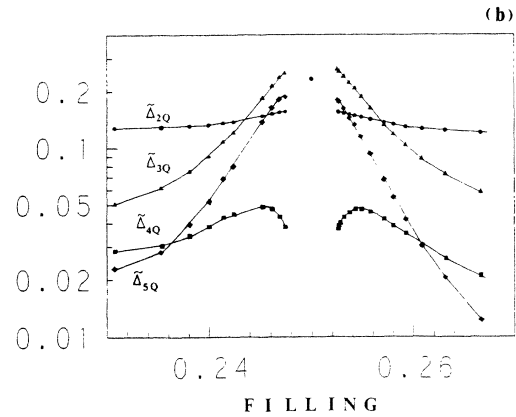
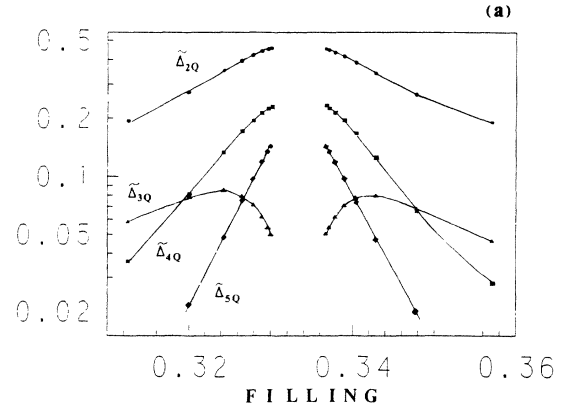


FIG. 10. Variation of various higher harmonics normalized by the corresponding fundamental order parameter: $\tilde{\Delta}_{lQ} \equiv \Delta_{lQ}/\Delta_Q$ as a function of the electron filling. (a) The third-filled case ($\alpha=1.08$), (b) the quarter-filled case ($\alpha=1.08$), and (c) the half-filled case ($\alpha=0.9$).

the $+--$ pattern becomes $--+$. A phase change of $\pm 2\pi/3$ occurs, depending upon $\delta \gtrless 0$. In the $\frac{1}{4}$ -filled case the phase change is $\pm \pi/2$.

Figure 14 shows the local electron density averaged over a few neighboring sites. The excess (or deficit) electron from the third-filled band is accumulated at the kink site, accommodating a fractional charge of $2e/3$ per kink, including the electron spin. Note that the area under the curve in Fig. 14 is $\frac{1}{3}$. (The origin of the vertical scale is set to $\frac{1}{3}$.) The spatial extension of the excess (or

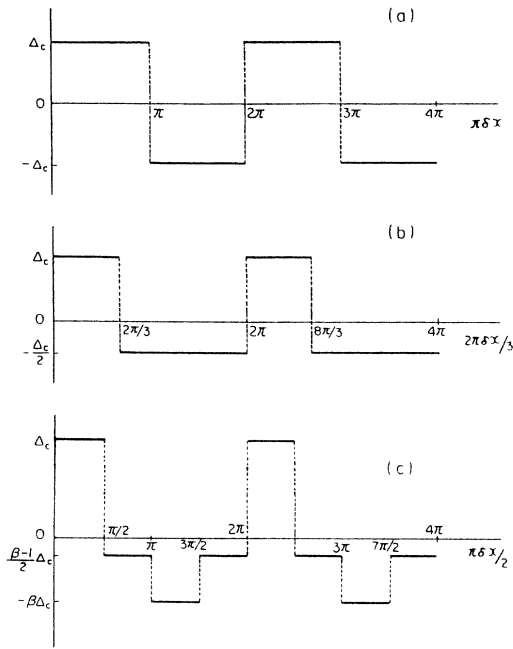


FIG. 11. Limiting forms of the envelope of the spatial modulation of the order parameters toward the commensurate state. Two periods of the spatial variation are drawn. (a) The half-filled case, (b) the third-filled case, and (c) the quarter-filled case, where β is a numerical factor which depends on the value of the higher harmonic: Δ_{2lQ} . (Note that if $\Delta_{2lQ}=0$, then $\beta=1$.)

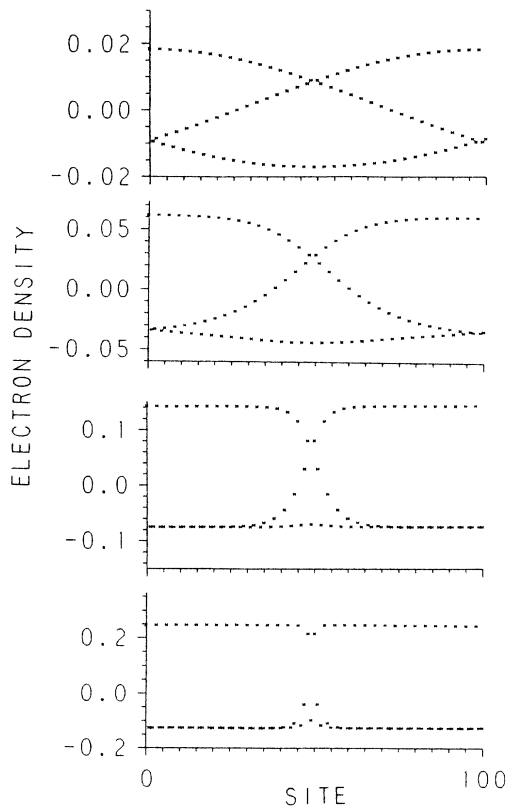


FIG. 12. Electron-density modulation in the nearly-third-filled case as a function of the site for various values of α ($\alpha=0.9, 1.0, 1.08$, and 1.15 from top to bottom with the same $\delta=\frac{1}{98}$). Since the modulation is periodic, we only display one period. As α increases, the width of a kink becomes narrower.

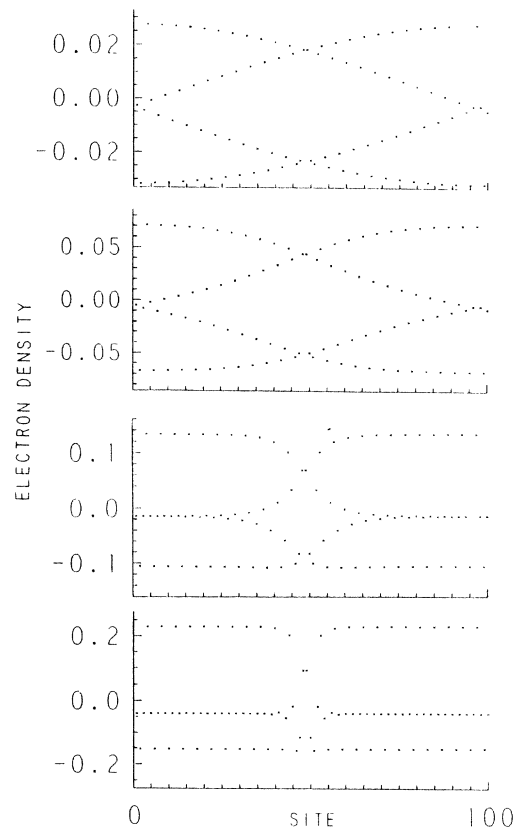


FIG. 13. Electron-density modulation in the nearly-quarter-filled case as a function of the site for various values of α ($\alpha=0.9, 1.0, 1.08$, and 1.15 from top to bottom, $\delta=-\frac{1}{97}$). One period of the periodic modulation is shown.

deficit) electron density approximately coincides with the width of a kink and becomes narrow as α increases. Except for the fact that the fractional charge per kink is $e/2$, the essential feature of the local-density modulation is same for the $\frac{1}{4}$ -filled case.

We note here the different roles played by the coupling constant α and the deviation δ from the nearby commensurate state in the formation of the kink lattice. While α determines the width of a kink, δ characterizes the spacing of the kink lattice as is clearly shown in Fig. 15 where the electron density is plotted by changing δ and keeping α fixed. Therefore even if α is small, the sharp kink lattice structure becomes clear as δ becomes small or the system enters a nearly commensurate state.

E. Wave functions

The amplitudes of the wave functions are shown in Fig. 16, indicating that the midgap state is localized exponentially at the kink site (see also Fig. 17) and its maximum is located precisely at the center of the kink, while those in the conduction (or valence) band are extended over a whole system. Thus the midgap state is responsible for the formation of the soliton.

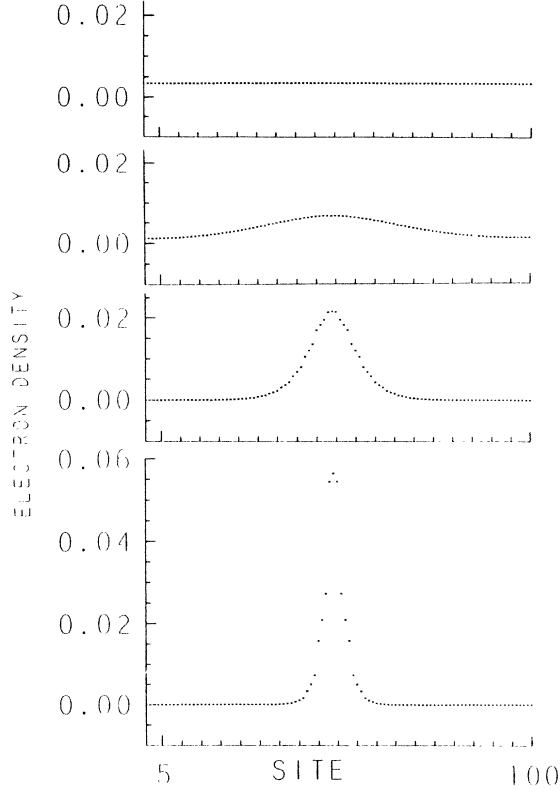


FIG. 14. Electron-density modulation averaged over a few neighboring sites in the nearly-third-filled case ($\alpha=0.9, 1.0, 1.08, \text{ and } 1.15$ from top to bottom with the same $\delta=\frac{1}{98}$). The origin of the vertical axis is set to the $\frac{1}{3}$ -filled case. Note that the area under the curve in each panel is $\frac{1}{3}$. As α increases, the excess electron density is seen to accumulate at the kink site.

IV. DISCUSSIONS

We have investigated various properties of the nearly commensurate CDW states and, in particular, studied the relative position and the width of the midgap band which appears inside the main Peierls energy gap. In this section we consider the possibility of observing such an energy-gap structure and examine the validity of our calculation.

A. Experimental relevance

The observation of the midgap band might be limited within the crossover region δ_{cr} , which we introduced in Sec. III C. We should point out that in this connection the ICDW materials usually have a lock-in transition from the incommensurate to commensurate state as the temperature decreases, just above which the system exhibits a nearly commensurate state. Therefore, if we adjust an appropriate temperature immediately above the lock-in transition, we always get a nearly commensurate situation in which the bandwidth of the midgap state is narrow enough to be easily accessible, experimentally. We pro-

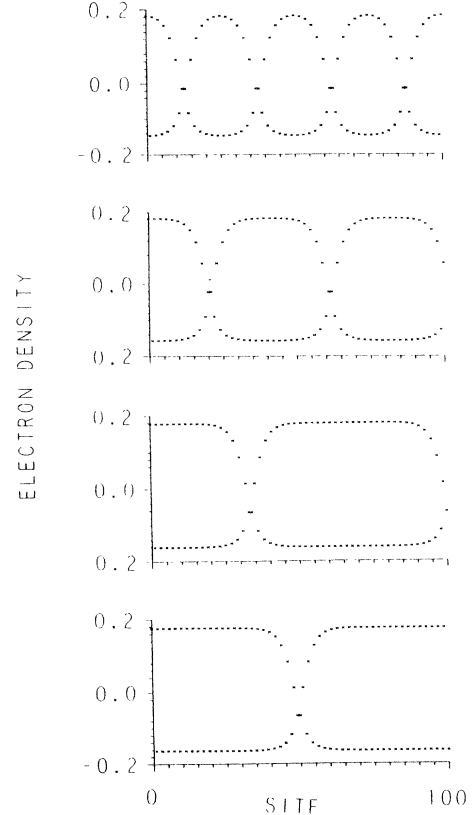


FIG. 15. Electron-density modulation in the nearly-half-filled case as a function of the site ($\delta=-\frac{1}{25}, -\frac{1}{41}, -\frac{1}{67}, \text{ and } -\frac{1}{99}$ from top to bottom with the same $\alpha=1.0$). As $|\delta|$ decreases, the region where the modulation is nearly commensurate is wider while the width of a kink is relatively unchanged.

pose experiments on various low-dimensional CDW materials such as $\text{K}_{0.3}\text{MoO}_3$ (Ref. 30) or $(\text{TaSe}_4)_2\text{I}$ (Ref. 31) to look for the midgap band. Optical-absorption or electron-tunneling measurements might be a direct way to detect it. In particular, in the former material the nearly-quarter-filled ICDW (Ref. 32) is realized at around 100 K. We believe that there exists a good chance to observe the midgap band in this material.

1. Remark on $\text{K}_{0.3}\text{MoO}_3$

As is mentioned above, $\text{K}_{0.3}\text{MoO}_3$ is a typical nearly-quarter-filled system. Fujishita *et al.*³¹ have concluded that there is a sinusoidal modulation of the ICDW state since they did not find higher-order satellites in the neutron diffraction experiment corresponding to the second harmonic Δ_{2Q} . We point out that the most important higher harmonic is not the second harmonic Δ_{2Q} but the third one, Δ_{3Q} , in the nearly-quarter-filled case, as is easily seen from Fig. 10(b). The former component (Δ_{2Q}) remains small while the latter (Δ_{3Q}) grows as the system approaches the nearly commensurate state. Therefore, we urge a precise diffraction experiment to see the CDW modulation.

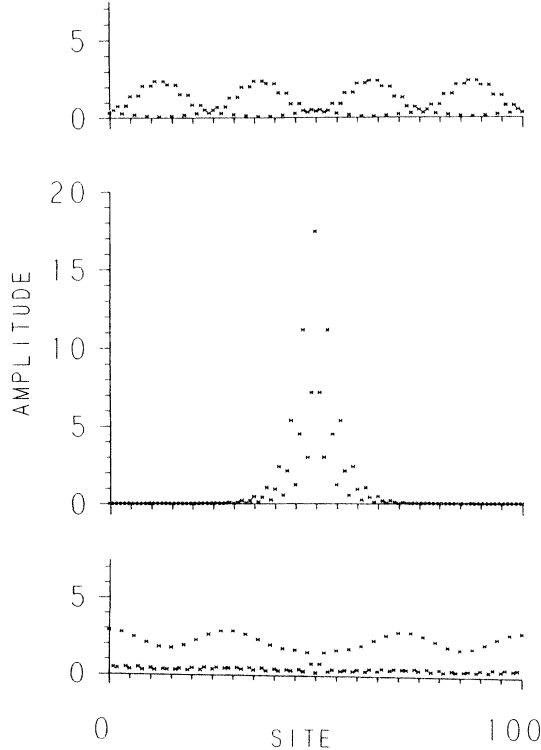


FIG. 16. Amplitude of the wave function in the third-filled case as a function of the site. The wave functions corresponding to the conduction (top) and valence (bottom) bands are extended. The wave function of the midgap band (middle) is localized around the kink site ($\alpha=1.15$ and $\delta=-\frac{1}{100}$).

2. Comments on NbSe₃

We mention here the work by Wilson³³ on NbSe₃, which is another nearly-quarter-filled system and exhibits two CDW transitions at $T_1=145$ K and $T_2=58$ K. By noticing that the two CDW wave numbers $Q_1=0.2408b^*$ and $Q_2=0.2599b^*$ along the chain axis can be well approximated by higher commensurate states, $Q_1=\frac{1}{4}(\frac{26}{27})b^*$ ($\cong 0.2407b^*$) and $Q_2=\frac{1}{4}(\frac{26}{25})b^*$ ($\cong 0.2600b^*$), he claims that the discommensuration (or

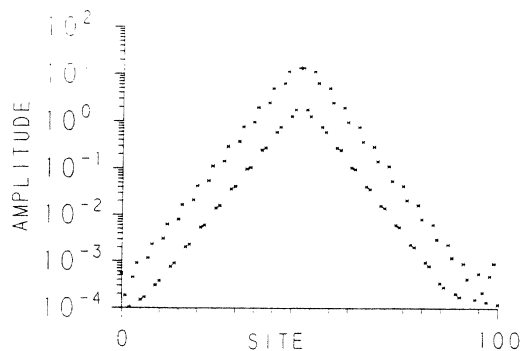


FIG. 17. Amplitude of the wave function of the midgap band in the quarter-filled case, indicating the localization with an exponential tail at the kink site ($\alpha=1.15$ and $\delta=\frac{1}{95}$).

kink) lattice structure characterizes the CDW in NbSe₃. The periods of the discommensuration lattices are 54 and 50 sites, corresponding to Q_1 and Q_2 , respectively. His assertion agrees with our model calculation. In fact, the experimental fact that the intensity of the second harmonic is very weak compared with that of the primary one associated with the wave number Q_1 is quite understandable in view of our theory.

3. Analysis of the experiment on TaS₃

Let us examine the experiments³ on another quasi-one-dimensional CDW system: orthorhombic TaS₃. The wave number⁴ of the ICDW along the chain axis or c axis continuously decreases from $\sim 0.255c^*$ at the onset temperature of the ICDW, $T_0 \cong 215$ K, to $0.250c^*$ at the lock-in commensurate-incommensurate (C-IC) transition temperature $T_{C-IC} \sim 90$ K. Therefore, orthorhombic TaS₃ is an ideal system with the nearly- $\frac{1}{4}$ -filled band ($\delta > 0$).

According to Itkis and Nad', the fundamental absorption spectrum at $T=98$ K just above the lock-in temperature consists of three peaks at $h\nu_1=184$ meV, $h\nu_2=125$ meV, and $h\nu_3=62$ meV. Since the energy of the $h\nu_1$ peak roughly coincides with the activation energy estimated from the conductivity measurement, we can identify it as the absorption across the main Peierls gap. As is seen from Fig. 7(b) [we note that the deviation δ from the quarter-filled-band in TaS₃ at 98 K is estimated as $\delta \cong 0$ (0.01)] we can expect two more absorptions in the ICDW state, namely the electronic transition from the occupied midgap state to the conduction band and the other transition from the valence band to the midgap state are expected. The applied electric field or thermal effect makes the latter process possible. We notice that $h\nu_1 - h\nu_2 \cong 59$ meV is roughly equal to $h\nu_3=62$ meV, coinciding with our assignment of the peaks. In the experimental data taken under other experimental conditions the essential feature mentioned above is preserved. Therefore we conclude that the ICDW in orthorhombic TaS₃ possesses a midgap state.

B. Validity of our calculation

1. Importance of higher harmonics

We show the band structure near the half-filled case by taking into account all harmonics in Fig. 18(a). The band structure is shown in Fig. 18(b) when only the odd harmonics ($\Delta_Q, \Delta_{3Q}, \dots$) which become relevant near the $\frac{1}{2}$ -filled case are taken into account and the even harmonics are neglected in the self-consistent calculation. We can see that the band structure for both cases remains almost the same, except that the midgap band is precisely situated at the center of the band in Fig. 18(b). Figure 19 exhibits the band structure when taking into account only the fundamental order parameter Δ_Q . The resulting bands are seen to be fragmented. Therefore, these results clearly indicate the importance of the effect of higher harmonics when we consider the stable lattice distortion and the energy-gap structure in the CDW systems. The ana-

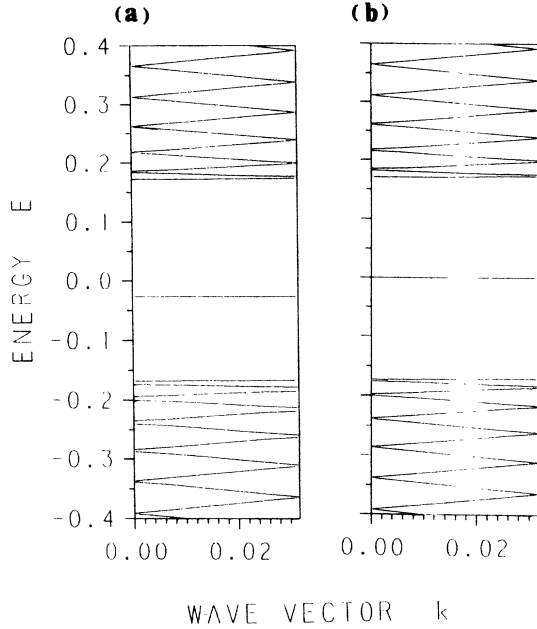


FIG. 18. Energy-gap structure near the Fermi level in the nearly-half-filled case ($\alpha=1.0$ and $\delta=\frac{1}{99}$). (a) All higher harmonics are considered. (b) Only odd harmonics are taken into account. Note that the midgap state is situated precisely at the middle of the band ($E=0$) in (b) while the overall gap structures in (a) and (b) are similar. Also see Fig. 19.

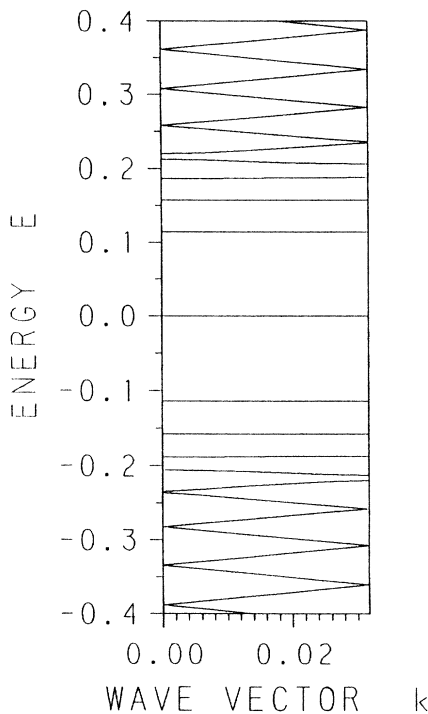


FIG. 19. Energy-gap structure near the Fermi level in the nearly-half-filled case ($\alpha=1.0$ and $\delta=\frac{1}{99}$), where only the fundamental component, Δ_0 , of the order parameter is taken into account. The band is fragmented. Compare with Figs. 18(a) and 18(b).

lytic solution,⁷⁻⁹ which takes into account only odd harmonics, corresponds to the situation in Fig. 18(b) and is valid in the limit of the nearly-half-filled case (or $|\delta|$ is very small); otherwise the even harmonics significantly affect various physical properties.

2. k -independent coupling constant

We have assumed that the electron-phonon coupling constant α introduced in Eq. (2.12) is independent of the wave number. Since in the nearly-half-filled case the relevant wave number is $Q=2k_F \cong \pi$, the wave-number-dependent coupling constants $\alpha_{(2l+1)Q}$ associated with the odd harmonics $\Delta_{(2l+1)Q}$ ($l=0,1,2,\dots$) are virtually same. Only one coupling constant α ($\equiv \alpha_Q$) is left. We note that the α_{2lQ} associated with the even harmonics Δ_{2lQ} , which tend to vanish, become irrelevant as the system approaches the commensurate state. The same argument holds for the nearly-third-filled case in which $(3l+1)Q$ is equivalent to $(3l+2)Q$, leaving only one relevant coupling constant α ($\equiv \alpha_Q$) because Δ_{3lQ} becomes irrelevant. Therefore, for these fillings we have essentially made no approximation on the k dependence of α .

In the nearly-quarter-filled case, however, we need two kinds of coupling constants, α_Q and α_{2Q} , because $(4l\pm 1)Q$ and $(4l\pm 2)Q$ are independent of each other, and $4lQ$ is irrelevant. Therefore, we have assumed $\alpha_Q = \alpha_{2Q} \equiv \alpha$ in this case. Since the order parameter Δ_{2Q} , whose amplitude does depend on the value of α_{2Q} , is less relevant than the primary order parameters $\Delta_{(4l+1)Q}$ and $\Delta_{(4l+3)Q}$, we believe that the essential feature we have drawn remains unchanged even if $\alpha_Q \neq \alpha_{2Q}$.

3. Validity of the assumption on periodic structures

In our analyses, the periodicity is assumed implicitly to coincide with the unit-cell size n (the commensurability

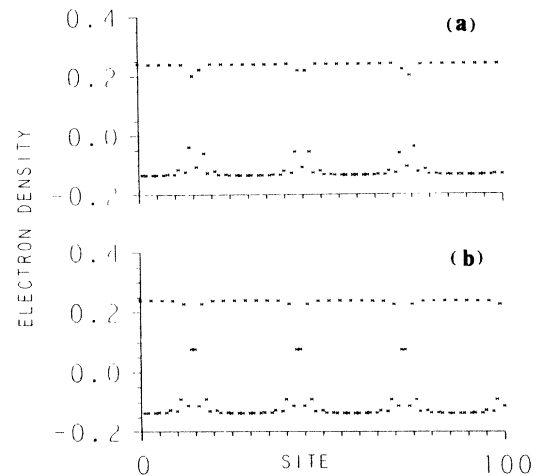


FIG. 20. Electron-density modulation in the nearly-half-filled case as a function of the site ($\alpha=1.15$). (a) The unit-cell size $n=90$ and $\delta=\frac{1}{30}$. (b) The unit-cell size $n=29$ and $\delta=\frac{1}{29}$. Note that despite the large difference of the unit sizes used the resultant modulations and band structures (Fig. 21) are quite similar.

index), by retaining selected Fourier components with wave number $2k_F$ and its higher harmonics. Furthermore, in all calculations discussed above, we fix the excess electron number per period to be $\pm\frac{1}{2}$, $\pm\frac{1}{3}$ or $\pm\frac{1}{4}$ in each filling, thus obtaining the soliton lattice structure in which the period is n sites and each soliton carries the corresponding number of electrons.

In order to check the stability of the structure, we make calculations with different number of excess electrons. For example (see Figs. 20 and 21), the nearly-third-filled system with $+1$ excess electron per 90 sites yields the same results as that with $+\frac{1}{3}$ excess electron per 29 sites. Notice that the periodic structure in Fig. 20(a) with unit cell size 30 is the computational result, not the assumed one. The associated band structures in Fig. 21 are very similar. The same situation occurs for other excess electron numbers and also for the nearly- $\frac{1}{2}$ -filled and nearly- $\frac{1}{4}$ -filled cases.

This proves the validity of the assumption on the periodicity (i.e., retaining only the harmonics of $2k_F$) and confirms the relative stability of those soliton lattice structures discussed in the previous sections.

V. SUMMARY AND CONCLUSION

We have given a detailed study of the midgap band found inside the main Peierls energy gap in the nearly commensurate state and proposed the limiting forms of the order parameters. We start with the Fröhlich model in one dimension within the mean-field approximation. Numerically diagonalizing the Hamiltonian matrices with sizes as large as 100×100 in a self-consistent manner and taking into account all higher harmonics of the CDW order parameter, we studied various properties of the nearly commensurate CDW states such as the energy-gap structure, the wave functions, and the electron-density distribution.

We mention other systems which exhibit the midgap state: The incommensurate spin-density-wave problem³⁴ in Cr is known to be equivalent mathematically to the present ICDW problem in the half-filled case. The midgap state in Cr is identified by optical reflectance measurement:³⁵ we have observed the midgap band absorp-

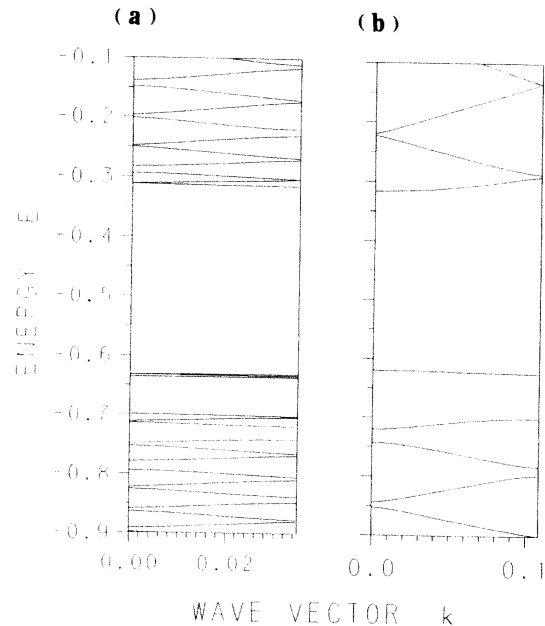


FIG. 21. Energy-gap structure near the Fermi level. A set of the parameters used is the same as in the corresponding Figs. 20(a) and 20(b). Energy-gap structures (the width of the main Peierls gap and the position of the midgap band) in (a) and (b) are very similar.

tion inside the main SDW gap. The coexistence phase of ferromagnetism and superconductivity in ErRh_4B_4 is interpreted³⁶ as the so-called Fulde-Ferrell state, which is also equivalent to the ICDW in the half-filled case. The electron-tunneling measurement by Lin *et al.*³⁷ exhibits a rich structure inside the superconducting energy gap, that is described in terms of the midgap state.³⁶

ACKNOWLEDGMENTS

The authors are much indebted to A. Kotani and I. Harada. Without their advice, the present work would not have been performed. Discussions with M. Fujita and T. Ohmi are gratefully acknowledged.

¹P. Bak, Rep. Prog. Phys. **45**, 587 (1982).

²See, for example, Wei-yi Wu, L. Mihály, G. Mozurkewich, and G. Grüner, Phys. Rev. Lett. **52**, 2382 (1984), and references therein.

³M. E. Itkis and F. Ya. Nad', Pis'ma Zh. Eksp. Teor. Fiz. **39**, 373 (1984) [JETP Lett. **39**, 448 (1984)].

⁴ZZ. Wang, H. Salva, P. Monceau, M. Renard, C. Roucau, R. Ayroles, F. Levy, L. Guemas, and A. Meerschaut, J. Phys. (Paris) Lett. **44**, L311 (1983).

⁵C. B. Kalem and N. P. Ong, Bull. Am. Phys. Soc. **30**, 312 (1985).

⁶W. P. Su, J. R. Schrieffer, and A. J. Heeger, Phys. Rev. Lett. **25**, 1968 (1979); Phys. Rev. B **22**, 2099 (1980).

⁷S. A. Brazovskii, S. A. Gordynin, and K. N. Kirova, Pis'ma Zh. Eksp. Teor. Fiz. **31**, 486 (1980) [JETP Lett. **31**, 456

(1980)].

⁸B. Horovitz, Phys. Rev. Lett. **46**, 742 (1981).

⁹J. Mertsching and H. J. Fischbeck, Phys. Status Solidi B **103**, 783 (1981).

¹⁰A. Kotani, J. Phys. Soc. Jpn. **42**, 408 (1977); **42**, 416 (1977).

¹¹J. A. Krumhansl, B. Horovitz, and A. J. Heeger, Solid State Commun. **34**, 945 (1980).

¹²W. P. Su and J. R. Schrieffer, Phys. Rev. Lett. **46**, 738 (1981).

¹³W. P. Su, Phys. Rev. B **27**, 370 (1983).

¹⁴J. T. Gammel and J. A. Krumhansl, Phys. Rev. B **27**, 7659 (1983).

¹⁵J. Hara and H. Fukuyama, J. Phys. Soc. Jpn. **52**, 2128 (1983).

¹⁶T. Ohmi and H. Yamamoto, Prog. Theor. Phys. **58**, 743 (1977).

¹⁷H. Yamamoto, I. Nakayama, and T. Ohmi, Prog. Theor.

- Phys. **59**, 351 (1978).
- ¹⁸J. Mertsching, Phys. Status Solidi B **113**, 609 (1982).
- ¹⁹H. J. Fischbeck, Phys. Status Solidi B **120**, 249 (1983); **125**, 275 (1984).
- ²⁰Y. Ono, Y. Ohfuti, and A. Terai, J. Phys. Soc. Jpn. **54**, 2641 (1985); also see S. Stafström, Phys. Rev. B **31**, 6058 (1985).
- ²¹H. J. Fischbeck, Phys. Status Solidi B **125**, 665 (1984).
- ²²Y. Ohfuti and Y. Ono, Solid State Commun. **48**, 985 (1983).
- ²³A. Kotani and I. Harada, J. Phys. Soc. Jpn. **49**, 535 (1980).
- ²⁴S. A. Brazovskii, N. E. Dzyaloshinskii, and I. M. Krichever, Zh. Eksp. Teor. Fiz. **83**, 389 (1982) [Sov. Phys.—JETP **56**, 212 (1982)].
- ²⁵W. P. Su, J. R. Schrieffer, and A. J. Heeger, Phys. Rev. Lett. **42**, 1698 (1979).
- ²⁶P. Y. Le Daéron and S. Aubry, J. Phys. (Paris) Colloq. **44**, C3 1573 (1983).
- ²⁷The requirement of self-consistency makes our problem quite distinct from the spectrum problem of the almost periodic Schrödinger operator. See, for example, R. E. Prange, D. R. Grempel, and S. Fishman, Phys. Rev. B **29**, 6500 (1984); M. Kohmoto, L. P. Kadanoff, and C. Tang, Phys. Rev. Lett. **50**, 1870 (1983).
- ²⁸A preliminary report of this work has been published [K. Machida and M. Nakano, Phys. Rev. Lett. **55**, 1927 (1985)].
- ²⁹M. Fujita, M. Nakano, and K. Machida (private communication).
- ³⁰M. Sato, H. Fujishita, and S. Hoshino J. Phys. C **16**, L877 (1983); D. C. Johnston, Phys. Rev. Lett. **52**, 2049 (1984); R. M. Fleming, L. F. Schneemeyer, and D. E. Moncton, Phys. Rev. B **31**, 899 (1985).
- ³¹C. Roucau, R. Ayroles, P. Gressier, and A. Meerschaut, J. Phys. C **17**, 2993 (1984); H. Fujishita, M. Sato, S. Sato, and S. Hoshino, *ibid.* **18**, 1105 (1985); D. C. Johnston, M. Maki, and G. Grüner, Solid State Commun. **53**, 5 (1985); K.-B. Lee, D. Davidov, and A. J. Heeger, *ibid.* **54**, 673 (1985).
- ³²Strictly speaking, the electron filling is nearly $\frac{3}{4}$ in $\text{K}_{0.3}\text{MoO}_3$. However, the essential feature of the one-quarter-filled case does not change due to the particle-hole symmetry.
- ³³J. A. Wilson, Phys. Rev. B **19**, 6456 (1979); J. Phys. F **12**, 2469 (1982).
- ³⁴K. Machida and M. Fujita, Phys. Rev. B **30**, 5284 (1984).
- ³⁵K. Machida, M. A. Lind, and J. L. Stanford, J. Phys. Soc. Jpn. **53**, 4020 (1984).
- ³⁶K. Machida and H. Nakanishi, Phys. Rev. B **30**, 122 (1984).
- ³⁷L.-J. Lin, A. M. Goldman, A. M. Kadin, and C. P. Umbach, Phys. Rev. Lett. **51**, 2151 (1983).